Building Simulation

Seventh International IBPSA Conference
Rio de Janeiro, Brazil
August 13-15, 2001

ANALYSING MULTIVARIABLE CONTROL OF REFRIGERATION PLANT USING MATLAB/SIMULINK

C P Underwood

University of Northumbria
Newcastle upon Tyne NE1 8ST, United Kingdom

ABSTRACT

Little work has been done on the closed loop response of refrigeration plant using the new chlorine-free refrigerants. A simulation model of a water-water refrigeration plant using R134a is developed for the purpose of investigating control system performance. The well-established problem of coupling between the two main regulatory control loops governing evaporator degree-of-superheat and plant capacity is recognised and the two control loops are tuned in harmony using an optimisation technique. To test the applicability of the control system design, the tuned controllers are applied to an identical plant but this time using the zeotrope R407C. Results show that the two control loops can be satisfactorily tuned to give minimal interaction and that the choice of working fluid has minimal effect on plant behaviour.

INTRODUCTION

Since the key work of James and Marshall (1973) which considered the dynamics of an R12-based water-water refrigeration plant including thermostatic capacity controls, comparatively little has been done on whole plant dynamics and control. Sami and Duong (1991) investigated heat pump system dynamic characteristics using refrigerant R134a (water-water and water-air) as an open loop problem in the absence of control and compared this with the (now banned) refrigerant R12. Votsis *et al* (1991) looked at the performance of a controlled residential heat pump system during the crucial start-up phase using an experimental rig resulting in a simple overall expression to describe the response of the plant during this phase only. At a more rigorous level of modelling, a number of workers have dealt with individual components of the plant such as Nyers and Stoyan (1992) who investigated evaporators, and Judge and Radermacher (1997) who looked at air-to-refrigerant evaporators and condensers. The only comprehensive work that has taken account of all regulatory control loops in a "whole plant" context is due to He *et al* (1998) who developed a reasonably simple simulation model of a residential scale air-water air conditioner. They used this to develop a linearised state-space model of the plant with which they used state observer theory to develop robust de-coupled control over evaporator superheat and plant capacity. Indeed they were among the first to recognise and attempt to remedy the problems associated with interaction in these two control loops, though the tendency for expansion device "hunting" has been known about for some time (Broersen and van der Jagt (1980)).

In this work, the dynamic response of the larger medium scale water-water plant is investigated with reference to control system design. A simulation model is developed and the two interacting loops are tuned in harmony using a gradient-based optimisation method in order to arrive at overall plant response with minimal loop interaction. Based initially on refrigerant R134a, the newer zeotrope R407C is also included in order to establish any further complications in the control of plants using this fluid due to its non-isothermal boiling and condensing behaviour.

Of particular interest from a modelling and simulation viewpoint is the use of a toolbox-based optimisation method that runs in tandem with the simulation thus expanding the utility of the simulation itself.

MODELLING

A general schematic of the plant is shown in Figure 1. Each heat exchanger is treated as a single zone lumped capacity and momentum effects are neglected. With this "stirred tank" philisophy, thermofluid properties (i.e. temperature/enthalpy; density) within each modelling zone are assumed to be equal to the outlet conditions. Thus energy and continuity balances for the evaporator, condenser and accumulator can be expressed in the following general form:

Energy,

$$\dot{T}_{wo} = [m_w cp_w (T_{wi} - T_{wo}) \pm q_w] / C_w \quad [1]$$

$$\dot{T}_m = [\pm q_w \pm q_r] / C_m \quad [2]$$

$$\dot{h}_{ro} = [m_r h_{ri} - m_r h_{ro} \pm q_r] / M_r \quad [3]$$

$$q_r = A U_r (\pm T_m \pm T_r) \quad [4]$$

$$q_w = A U_w (\pm T_m \pm T_{wo}) \quad [5]$$

Continuity,

$$\dot{M}_r = m_{ri} - m_{ro} \quad [6]$$

$$\rho_r = M_r / V_r \quad [7]$$

The mass flow rate of refrigerant handled by the compressor was taken to be,

$$m_r = u V_v \rho_{ri} (1 - V_v / V_d) \left[(P_c / P_e)^{1/n} - 1 \right] \quad [8]$$

Finally, thermodynamic properties of the refrigerant,

$$T_{rs} = f(\rho_r) \quad [9]$$

$$cp_{rg}, h_{rs}, P = f(T_{rs}) \quad [10]$$

$$T_{rg}, x_r = f(h_r, h_s, T_{rs}, cp_{rg}) \quad [11]$$

Waterside surface heat transfer coefficients were calculated using the Gnielinski/Petukov (e.g. Holman (1997a)) correlation (for water flowing within the condenser tubes) and the Grimson (e.g. Holman (1997b)) correlation (for water flowing over the evaporator tubes). Both values were taken to be constant. On the refrigerant side, the following was derived for flow boiling heat transfer of R134a in the smooth evaporator tubes based on the mean of data collected from Zürcher *et al* (1998), Eckels and Pate (1991) and Lallemand *et al* (2001):

$$U_{re} = -1.802 + 3.012 \times 10^{-2} F_{re} - 3.225 \times 10^{-5} F_{re}^{\ 2} \quad (0.1 < x_{re} < 0.9) \quad [12]$$

However, it was noted that little progress has been made on flow condensation over smooth tube banks particularly for the newer chlorine-free refrigerants and their blends, such as is the case in the condenser. Thus the following simple general expression was used in the present study (Collier and Thome (1996)):

$$Nu_{rc} = 0.9 Re_{rf}^{\ 1/2} \quad [13]$$

The above is evaluated at saturated liquid conditions and is applicable for the lower liquid Reynold's numbers at which flow separation is not expected to be a feature.

Interpretation of the Model Equations

For the evaporator and condenser, the "stiff" influence of the zone enthalpy equation (eqn. 3) was relaxed to give a steady-state refrigerant side heat balance. For the evaporator, eqn. 3 was thus re-arranged to obtain outlet enthalpy (normally superheated) whereas for the condenser the outlet state was assumed to be saturated at all times and eqn. 3 was thus re-arranged to yield outlet mass flow rate. For the accumulator, clearly only eqn. 3 is relevant as far as energy is concerned and in this case $q_r = 0$. As to continuity, in eqn. 7 the refrigerant zone density was obtained by treating the zone volume as a constant in the cases of the evaporator and condenser, whereas the variable refrigerant volume was obtained from this equation for the accumulator. The liquid density used in the latter was obtained from the condenser continuity equation.

A refrigerant property routine was written as a Matlab function (i.e. eqns. 9-11). This was based

on the Extended Antoine Equation (ICI Klea (1996)) for the equilibrium pressure/temperature state. The resulting implicit scheme was solved within the Matlab function using an interval-halving convergence algorithm.

Positioning Mechanisms and Controllers

In the present work, compressor control is based on a variable speed drive, the position of which was assumed to lag the incoming positioning signal according to a first order lag. An adapted form of the second-order expansion device model proposed by Broersen and ten Napel (1982) was used. Since their model was based on a direct-acting mechanical valve (whereas in the present work an electronic expansion device is used), the two dominant dynamics involved (i.e. the positioning mechanism and the measurement of the degree-of-superheat) were split up. Hence the valve position was taken to follow a linear characteristic, lagging the incoming control signal according to a first order lag with a time constant assumed to be the same as that proposed by Broersen and ten Napel (1982) – 16.2s. The degree-of-superheat measurement on the other hand was also treated as a first order lag with a time constant of 5s, consistent with typical sheathed immersion type resistance temperature detectors or thermocouples.

Finally, the model was completed with control loop closure comprising 2 proportional-plus-integral-plus-derivative (PID) controllers governing plant capacity (via evaporator leaving chilled water temperature) and degree-of-superheat.

Model Construction and Solution

The model was implemented in Matlab/Simulink (Mathworks (2000)). The mostly non-linear differential equations (i.e. eqns. 1,2,3 and 6) were interpreted in Simulink using the template shown in Figure 2. Thus the overall plant model of Figure 3 was developed in which the main component equation sets are formed into 3 masked subsystems for convenience. The solution scheme chosen was a variable step stiff-trapezoidal method from the Simulink solver library. This proved to be reasonably efficient, solving a typical 500s simulation time span in under 60s (much of the effort being due to the parsing of data to and from the two Matlab functions used for the solution of evaporator and condenser refrigerant states).

Application

The model was applied to a typical small-scale water chiller of 60kW nominal refrigerating effect. Physical dimensions from which heat exchange areas and thermal capacities, etc were obtained were taken from typical manufacturer data. Boundary data and initial conditions were set as follows:

Evaporator:	Rated capacity: 60kW
	Inlet water temperature: 10°C
	Outlet water temperature: 7°C
	Evaporating temperature: 0°C
Compressor:	Swept volume: 5.3135×10^{-2} m^3
	Displ. volume: 2.5954×10^{-3} m^3
	Minimum turndown: 20%
	Nom. mass flow rate: 0.455kgs^{-1}
Condenser:	Rated capacity: 78kW
	Inlet water temperature: 30°C
	Outlet water temperature: 40°C
	Condensing temperature: 45°C

CONTROL SYSTEM TUNING

The model was first applied to the tuning of the two controllers, governing plant capacity and degree-of-superheat. This was achieved through the application of two Simulink Non-linear Control Design Blocksets (NCD) as shown in the model layout of Figure 3.

The NCD block works as follows. A constraint envelope is defined that fixes upper and lower bounds of the controlled variable, together with a number of tunable variables (4 in this case – the proportional and integral gains of both controllers). A cost function is generated consisting of a weighted maximum constraint violation. At each iteration, each tunable variable is perturbed in turn and the resulting constraint values and cost function are evaluated. A gradient search direction is determined from these results and a line search along the gradient is performed in order to minimise the cost function while simultaneously satisfying the constraint envelope criteria.

The optimisation was implemented as follows:

a) Set point changes in evaporator leaving water temperature were introduced and the NCD blocks adjusted the tunable variables until the constraint envelop criteria were met. Thus set point following in the plant capacity loop and disturbance rejection in the degree-of-superheat loop were optimised.
b) The process was repeated but this time with set point changes introduced to the degree-of-superheat loop, thus optimising for disturbance rejection in the plant capacity loop and set

point following in the degree-of-superheat loop.

An example of a constraint envelope used (in this case for capacity set point tracking) is shown in Figure 4. In practice a range of tunable variable values is obtained within which the optimised plant performance lies for a range of disturbances and command inputs. In the present study, variations in the tunable variable results were minimal and a reasonable set of mean values were obtained as follows:

$$K_1 = -0.5\mathrm{K}^{-1}\ ;\ I_1 = -0.017(\mathrm{Ks})^{-1}$$
$$K_2 = 4\mathrm{K}^{-1}\ ;\ I_2 = 0.133(\mathrm{Ks})^{-1}$$

Note that the derivative controller terms were not tuned in the present study. In practice, the range of values might be accounted for in relation to all plant operating modes by the introduction of gain scheduling as was used by He *et al* (1998) in their analysis. Results based on the above are shown in Figure 5 for set point changes of 7-8.5°C in evaporator outlet water temperature (i.e. halving of plant capacity) and 5-2.5K in degree-of-superheat. Evidently, degree-of-superheat disturbance arising from action in the plant capacity loop is minimal whereas plant capacity disturbance arising from action in the degree-of-superheat loop is more pronounced. In general however, both loops perform well with a good degree of robustness.

R407C PLANT

One of the objectives of this study was to compare the performance of the plant under control based on the pure refrigerant R134a, with an identical plant using the increasingly commonly used zeotrope R407C. The reason for this was to establish whether the non-isothermal boiling and condensing conditions with the zeotrope was likely to have any impact on plant performance under control. The model was adjusted in a number of respects:

a) New thermodynamic property routines had to be developed for refrigerant R407C (ICI Klea (1995)). These were characterised by the return of a dew point temperature and a bubble point temperature in place of the essentially constant saturation temperature of the pure refrigerant case.
b) Refrigeration saturation temperature was replaced with the mid-envelope temperature for all heat transfer calculations. The mid-envelope temperature was taken to be the mean of the bubble point and dew point temperatures for the given process.
c) The calculation of evaporator degree-of-superheat conditions required to be changed with reference to dew point temperature instead of saturation temperature.

Zürcher *et al* (1998) noted a close similarity between their flow boiling correlations for both R134a and R407C and thus it was unnecessary to redefine eqn. 12 for the boiling heat transfer coefficient. In all other respects, the R407C plant was taken to be the same as the R134a plant, including the control system specification.

LOAD TRACKING RESULTS

Load tracking for both R134a and R407C plants was investigated by disturbing the chilled water inlet temperature to the evaporator using a square wave. Results are shown in Figure 6. Both plants recover to set point well after the two discrete disturbances in load. The R407C plant is noted to be slightly less stable than the R134a plant at the same controller specification.

CONCLUSIONS

A dynamic thermal model for water-water refrigeration plant is described for the purpose of investigating control system tuning and performance. The interacting MIMO control system is tuned in harmony using a gradient-based optimisation technique and results showing good disturbance and command tracking with a good degree of robustness were obtained. Plant performance based on refrigerants R134a and R407C are compared and both give good load disturbance tracking though the R407C plant is slightly less stable than the R134a plant when using an identical control system specification. Further work is warranted on mechanisms for the adaptation of the controller specification to a wider range of operating conditions and working fluid types likely to be found in practice.

REFERENCES

Broersen P M T and van der Jagt M F G (1980) Hunting of Evaporators Controlled by a Thermostatic Expansion Valve *ASME Trans: J. Dynamical Systems* 102 130-135

Broersen P M T and ten Napel J (1982) Identification of a Thermostatic Expansion Valve *IFAC Symposium on Identification and System Parameter Estimation* 415-420 Washington

Collier J G and Thome J R (1996) *Convective Boiling and Condensation* pp467-468 (Oxford: Oxford University Press)

Eckels S J and Pate M B (1991) An Experimental Comparison of Evaporation and Condensation Heat Transfer Coefficients for HFC-134a and CFC-12 *Int. J. Refrig.* 14(3) 70-77

He X-D, Liu S, Asada H H and Itoh H (1998) Multivariable Control of Vapour Compression Systems *Int. J. HVAC&R Res.* 4(3) 205-230

Holman J P (1997a) *Heat Transfer* p289 (New York: McGraw-Hill)

Holman J P (1997a) *Heat Transfer* p311 (New York: McGraw-Hill)

ICI Klea (1996) *Physical Property Data Sheet: R134a* (Runcorn: ICI Klea)

ICI Klea (1995) *Physical Property Data Sheet: R407C* (Runcorn: ICI Klea)

James R W and Marshall S A (1973) Dynamic Analysis of a Refrigeration System *Proc. Inst. Refrig.* 70 13-24

Judge J and Radermacher R (1997) A Heat Exchanger for Mixtures and Pure Refrigerant Cycle Simulations *Int. J. Refrig.* 20(4) 244-255

Lallemand M, Branescu C and Haberschill P (2001) Coefficients d'échange locaux au cours de l'ébullition du R22 et du R407C dans des tubes horizontaux, lisse ou micro-ailetté *Int. J. Refrig.* 24 57-72

Mathworks (2000) *SIMULINK – Dynamic System Simulation for MATLAB* (Natick: The Mathwo rks Inc)

Nyers J and Stoyan G (1992) A Dynamical Model Adequate for Controlling the Evaporator of a Heat Pump *Int. J. Refrig.* 17(2) 101-108

Sami S M and Duong T N (1991) Dynamic Performance of Heat Pumps using Refrigerant R134a *ASHRAE Trans.* 97(2) 41-47

Votsis P P, Tassou S A, Wilson D R and Marquand C J (1991) Dynamic Characteristics of an Air-to-water Heat-pump System *Int. J. Refrig.* 15(2) 89-94

Zürcher O, Thome J R and Favrat D (1998) In-tube Boiling of R-407C and R-407C/Oil Mixtures – Part II: Plain Tube Results and Predictions *Int J. HCAC&R Res.* 4(4) 373-399

NOMENCLATURE

A	Surface area (m^2)
C	Thermal capacity (kJK^{-1})
cp	Specific heat capacity ($kJkg^{-1}K^{-1}$)
f	A function of…
F	Refrigerant mass flux ($kgm^{-2}s^{-1}$)
h	Specific enthalpy ($kJkg^{-1}$)
I_1	Capacity loop integral gain ($K^{-1}s^{-1}$)
I_2	Superheat loop integral gain ($K^{-1}s^{-1}$)
K_1	Capacity loop controller gain (K^{-1})
K_2	Superheat loop controller gain (K^{-1})
m	Mass flow rate (kgs^{-1})
M	Mass (kg)
n	Index of compression (taken to be 1.3)
Nu	Nusselt number
P	Pressure (bar)
q	Heat transfer rate (kW)
Re	Reynolds number
ρ	Density (kgm^{-3})
T	Temperature(K, ^oC)
u	Control signal ($0 \le u \le 1$)
U	Heat transfer coeff. ($kWm^{-2}K^{-1}$)
V	Volume (m^3)
x	Refrigerant quality

Subscripts:

c	Refers to condenser
d	Displacement (volume)
e	Refers to evaporator
f	Liquid state
g	Gaseous state
i,o	Inlet, outlet
m	Material (i.e. heat exchanger metal)
r	Refrigerant
s	Saturated state
v	Swept (volume)
w	Water

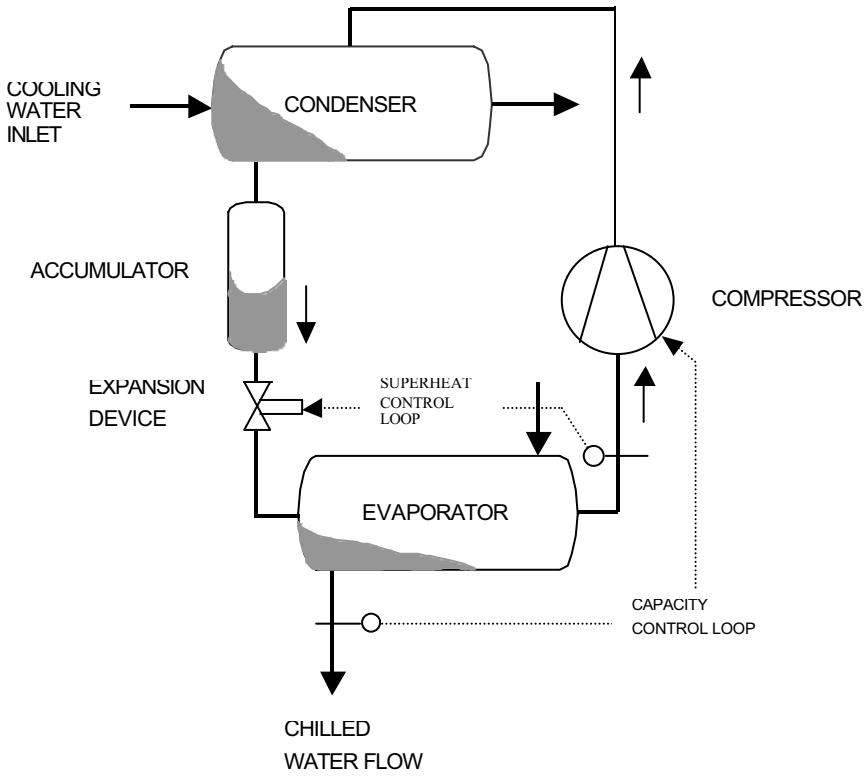

Figure 1: Schematic Layout of the Plant

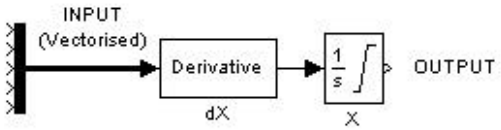

Figure 2: Simulink Template for the Differential Equations

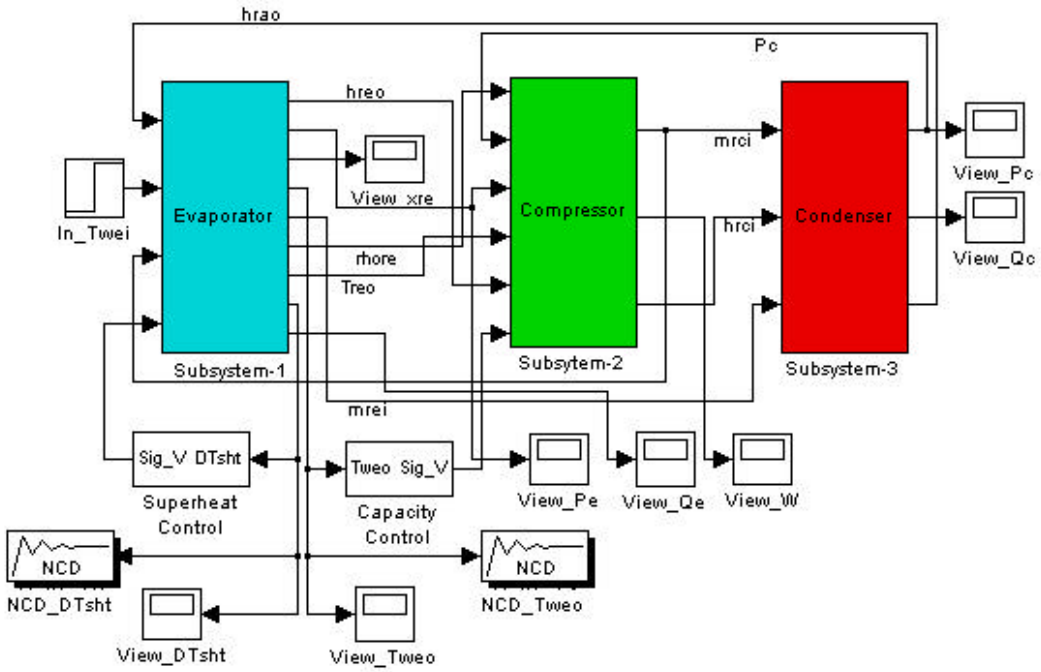

Figure 3: Simulink Model of the Plant

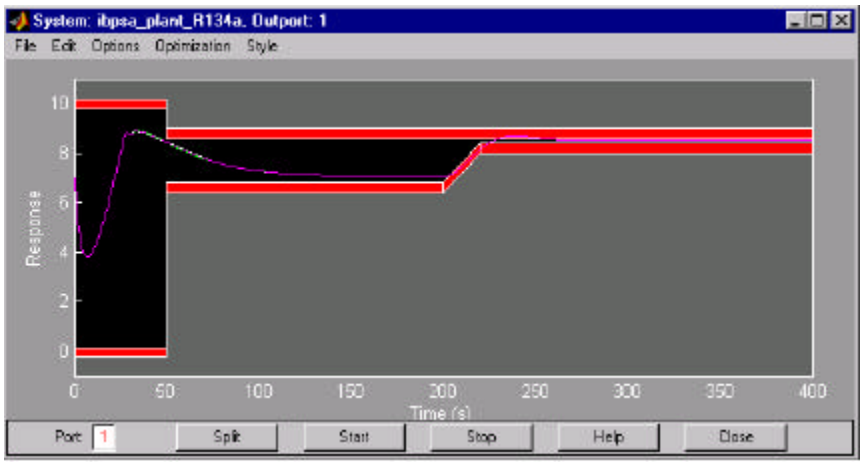

Figure 4: Constraint Envelope – Capacity Command Tracking

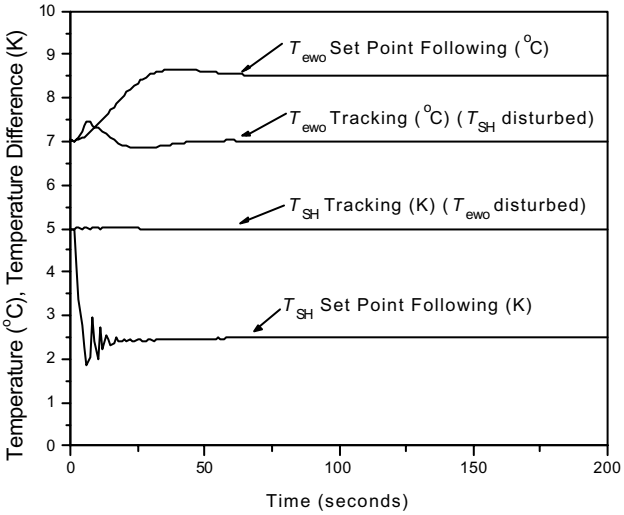

Figure 5: Simulated Tuning Responses

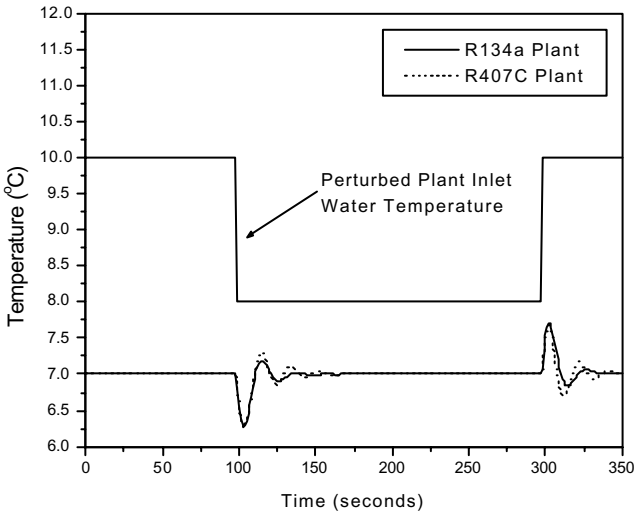

Figure 6: Simulated Load Tracking Response